Crystal structure of the temperature-sensitive and allosteric-defective chaperonin GroELE461K

ARTICLE *in* JOURNAL OF STRUCTURAL BIOLOGY · OCTOBER 2006

Impact Factor: 3.23 · DOI: 10.1016/j.jsb.2006.06.008 · Source: PubMed

Available online at www.sciencedirect.com
ScienceDirect
Journal of Structural Biology 155 (2006) 482–492
Journal of Structural Biology
www.elsevier.com/locate/yjsbi

Crystal structure of the temperature-sensitive and allosteric-defective chaperonin $GroEL_{E461K}$

Aintzane Cabo-Bilbao [a], Silvia Spinelli [b], Begoña Sot [a], Jon Agirre [a], Ariel E. Mechaly [a], Arturo Muga [a], Diego M.A. Guérin [a,c,*]

[a] *Unidad de Biofísica (CSIC-UPV/EHU), P.O. Box 644, E-48080 Bilbao, Spain*
[b] *AFMB-CNRS, UMR 6098. 163, Av. de Luminy, 13288 Marseille Cedex 09, France*
[c] *Departamento de Física, Universidad Nacional del Sur, Bahía Blanca, Argentina*

Received 16 March 2006; received in revised form 16 June 2006; accepted 27 June 2006
Available online 8 July 2006

Abstract

The chaperonin GroEL adopts a double-ring structure with various modes of allosteric communication. The simultaneous positive intra-ring and negative inter-ring co-operativities alternate the functionality of the folding cavities in both protein rings. Negative inter-ring co-operativity is maintained through different inter-ring interactions, including a salt bridge involving Glu 461. Replacement of this residue by Lys modifies the temperature sensitivity of the substrate-folding activity of this protein, most likely as a result of the loss of inter-ring co-operativity. The crystal structure of the mutant chaperonin $GroEL_{E461K}$ has been determined at 3.3 Å and compared with other structures: the wild-type GroEL, an allosteric defective GroEL double mutant and the GroEL–GroES-$(ADP)_7$ complex. The inter-ring region of the mutant exhibits the following characteristics: (i) no salt-bridge stabilizes the inter-ring interface; (ii) the mutated residue plays a central role in defining the relative ring rotation (of about 22°) around the 7-fold axis; (iii) an increase in the inter-ring distance and solvent accessibility of the inter-ring interface; and (iv) a 2-fold reduction in the stabilization energy of the inter-ring interface, due to the modification of inter-ring interactions. These characteristics explain how the thermal sensitivity of the protein's fundamental properties permits GroEL to distinguish physiological (37 °C) from stress (42 °C) temperatures.

Keywords: GroEL; E461K; Co-operativity; Chaperonin

1. Introduction

The GroEL–GroES chaperonin complex helps unfolded polypeptides to achieve the active conformation via a nucleotide-regulated cyclic reaction. GroEL is a double-heptameric 800 kDa toroid made of identical subunits that contains a central cavity. GroES is a dome-like 70 kDa homo-heptamer that binds to the same GroEL ring to which other ligands (non-native polypeptides and nucleotides) are already bound. In this way, the complex GroES–GroEL forms a hydrophobic cavity where the peptide searches for the productive structure in an isolated environment, known as the Anfinsen cage, and is subsequently returned to the medium.

Each GroEL subunit is composed of three domains: (1) an apical domain (186 residues) that interacts with non-folded substrate proteins and GroES; (2) an intermediate domain (89 residues) that forms the outer wall of the cylinder and provides a flexible covalent connection from the apical to the equatorial domain; and (3) the equatorial domain (243 residues), which in addition to securing the nucleotide binding site, yields most of the intra-ring and all of the inter-ring contacts (Bartolucci et al., 2005; Braig et al., 1994). GroES binding to the ATP-bound ring induces major conformational changes in the apical and intermediate

* Corresponding author. Present address: Unidad de Biofísica (CSIC-UPV/EHU), Barrio Sarriena S/N, 48940 Leioa, Vizcaya, Spain. Fax: +34 946013360.
E-mail address: diego.guerin@ehu.es (D.M.A. Guérin).

1047-8477/$ - see front matter © 2006 Elsevier Inc. All rights reserved.
doi:10.1016/j.jsb.2006.06.008

domains. The ability of the GroEL–GroES complex to form an asymmetric arrangement stems from sophisticated allosteric regulation of the protein by ATP. As seen in binding and hydrolysis studies, GroEL displays positive intra-ring and negative inter-ring co-operativity (Yifrach and Horovitz, 1995). In light of the protein's double-ring structure, the combination of both allosterism types implies that there are two, TT and TR (Inobe et al., 2003) or three, TT, TR, and RR (Aharoni and Horovitz, 1996) allosteric states. In this model, T and R represent the allosteric state of each ring, with T corresponding to high affinity for substrate proteins and low affinity for ATP, and R corresponding to low affinity for peptide substrates and high affinity for ATP.

The importance of negative inter-ring allosterism in the functional cycle of GroEL is highlighted by the fact that the co-operative binding of ATP to the *trans* ring promotes dissociation of GroES from the *cis* ring, which in turn leads to diffusion of the substrate protein, once it is properly folded. Despite the well-recognized importance of this allosteric level in the biological function of GroEL, the molecular interactions that mediate inter-ring signalling are not well understood. The 3D structure of apo wild-type GroEL protein (Bartolucci et al., 2005; PDB code: 1XCK) and that of the asymmetric complex GroEL–GroES-$(ADP)_7$ (Xu et al., 1997; PDB code: 1AON) reveal that each subunit interacts with two subunits of the opposite ring via two contact sites, named after Braig (Braig et al., 1994) *left* and *right* contact sites. This sites are stabilized by both hydrophobic and electrostatic interactions. Salt bridge E461–R452 at the *right* contact site is believed to form part of the so-called *thermosensor* that allows GroEL to distinguish physiological (37 °C) from stress (42 °C) temperatures (Sot et al., 2002). In fact, disruption of the E461–R452 ionic contact results in a reduction of (i) the temperature at which the inter-ring negative co-operativity and refolding activity of the protein disappear (Sot et al., 2002); (ii) protein stability against thermal challenge (Sot et al., 2003); and (iii) positive intra-ring co-operativity (Sewell et al., 2004).

In previous papers we also observed that the number of ionic contacts at the inter-ring interface is an important factor in controlling negative co-operativity in GroEL. Decreases in the number of ionic pairs at this interface increased inter-ring spacing and weakened inter-ring communication (Sot et al., 2002). Within this context, we also demonstrated that disruption of the inter-ring salt-bridges affected the ability of GroEL to distinguish physiological (37 °C) from stress temperatures (42–45 °C). $GroEL_{E461K}$ and $GroEL_{E434K}$ mutants, together with the co-chaperonin GroES, act at physiological temperatures (i.e., 37 °C) as storing devices preventing substrate release, a behaviour that wt GroEL displays at temperatures above 42 °C (Llorca et al., 1998; Sot et al., 2002).

To understand how the GroEL thermostat is programmed and to gain information about the signalling pathway associated with co-operativity in this protein, we determined the structure of $GroEL_{E461K}$ (2EU1) crystallized at 4 °C. Here, we describe the crystal structure of this mutant, which displays two major quaternary structural changes compared with other known *apo* and *holo* GroEL structures: the rings are rotated around the 7-fold axis, and the inter-ring spacing is increased. The structure of $GroEL_{E461K}$ allows us to examine in atomic detail these two major changes. The following sections are devoted to a detailed description of its structural and functional consequences.

2. Materials and methods

2.1. Protein expression and purification

GroEL mutants were produced using the homologous recombination technique (Martin et al., 1995), according to (Weissman et al. (1995)). Polymerase chain reaction was carried out using *Pfu* polymerase (Stratagene) on the plasmid pARGRO (Pérez-Pérez and Gutierrez, 1995). *Escherichia coli* GroEL was purified from a pAR3 plasmid harbouring a strain that over expresses the protein as previously described (Llorca et al., 1994).

2.2. Crystallization, data collection, and processing

Crystals of $GroEL_{E461K}$ were grown at 4 °C in hanging-drop vapour-diffusion experiments from drops (2 μl) containing a 1.5:1 (v/v) ratio of protein solution (22.5 mg/ml, in 50 mM Tris-acetate, 10 mM $MgCl_2$, pH 8.0) to well solution (43% (v/v) MPD, 100 mM imidazole, 170 mM $MgCl_2{\cdot}6H_2O$, pH 8.0). X-ray data were collected at the European Synchrotron Radiation Facility (ESRF), (Grenoble, France) with a loop-mounted crystal (Hampton), flash-frozen in liquid N_2 at 100 K, using an ADSC Q210 2D detector at beamline ID29. The data were indexed and integrated using the Denzo program (Otwinowky and Minor, 1997). Scaling and merging of the data, and the assignment the space group were done with SCALA from the CCP4 suite (Collaborative Computational Project, Number 4, 1994).

2.3. Structure solution, refinement, and analysis

The structure was solved by molecular replacement with the AMoRe program (Navaza, 1994) using a single ring (monomers A–G) from the double mutant (DM) GroEL R13G, A126V (1OEL, Braig et al., 1994; PDB code 1OEL) structure solved at 2.8 Å resolution (Braig et al., 1995) as a trial model. A solution was found when data collected with 15.0–4.0 Å resolution were included, with an R factor of 37%, a correlation coefficient of 73%, and inter-molecule/heptamer distance of 70.4 Å. This solution was refined with CNS (Adams et al., 1997; Brunger et al., 1998; Lee and Richards, 1971) until values of about 28.0 and 30.0 for R and R_{free} factors, respectively, were reached. The structure 1XCK was released and then their protein subunits individually superimposed to our refined model by minimizing the CA–CA distances. This new model was further refined up to the final parameters indicated in Table 1. Computations such as molecular rotations, calcula-

Table 1
$GroEL_{E461K}$ crystallographic data and refinement statistics

Diffraction data	
Unit cell dimensions (Å, °)	$a = 267.7$, $b = 290.6$, $c = 247.0$, $\alpha = \beta = \gamma = 90$
Space group	C2221
Resolution range (Å)	39.75–3.29
Measured reflections	123 350
Completeness of data (%)	85.4
R-stand(*F*)	0.110
Refinement statistics	
Used reflections	123 350
Resolution range (Å)	39.75–3.29
Total non-H protein atoms	53 984
Total water, ions, etc.	0
R factor/R_{free} factor (%)	27.6/29.6
r.m.s.d. bond length (Å)	0.011
r.m.s.d. bond angle (°)	1.33

R-stand(*F*) = $\langle\sigma(F)\rangle/\langle F\rangle$.
$R = \sum_{hkl} \|Fo_{hkl} - kFc_{hkl}\| / \sum_{hkl} Fo_{hkl}$.
R_{free} = *R*-value calculated for the 5% of reflections not used for refinement.

tion of NCS matrices, map extensions, mask calculation, and map averaging were also performed using the CCP4 suite. Models were built using the 'O' program (Jones et al., 1991). Structure refinement and F_o–F_c, *omit*, and $2F_o$–F_c map calculation, as well as computing inter-atomic distance and buried surfaces were performed with the CNS program (Adams et al., 1997; Brunger et al., 1998; Lee and Richards, 1971). The electron density inside the asymmetric unit was averaged taking the two rings separately. For each ring an envelope of a single monomer was constructed and seven rotation matrices computed by superimposing the seven equivalent monomers. Then, the electron density was averaged and the atomic model checked against it. During last refinement rounds a 7-fold NCS-restrain was applied among monomers within each ring (with group weight equal to 300), but leaving residues 29–34 unrestrained in order to evaluate whether Leu 31 was in the *cis* or *trans* conformation (see Section 3.5).

In order to minimize effects of local heterogeneities and of atomic model errors arising from data resolution limits, overall and averaged parameters, such as total inter-subunit contacts and monomer-averaged inter-atomic distances, were considered for structural comparison between GroEL models analyzed herein.

2.4. Images

Figures were generated using 'dino' (http://www.dino3d.org), 'gimp' (http://www.gimp.org), 'OpenOffice.org' (http://openoffice.org), and 'msms' (http://www.scripps.edu/~sanner/html/msms_home.html). *Solvent-excluded* surfaces of Figs. 1, 2 and 3 were computed with a probe radius of 1.4 Å.

In Figs. 3, 4 and 5, stick models were obtained by averaging the atomic coordinate values of all monomers of each ring after superposition by their equivalent CA-atoms. This was done by minimization of r.m.s.d. with program 'lsqkab' from the CCP4 suite (Collaborative Computational Project, Number 4, 1994).

Coordinates. Atomic coordinates and structure factors of $GroEL_{E461K}$ have been deposited in the RCSB Protein Data Bank with the accession code 2EU1.

3. Result and discussion

3.1. Structure of $GroEL_{E461K}$

Up to date, about 40 structures deposited in the Protein Data Bank are related to GroEL, most of them being different GroEL mutants in the *apo* as well as in complex forms. In order to analyse $GroEL_{E461K}$ mainly focusing on the inter-ring interface and temperature behaviour, we compared the mutant structure reported in this work with that of wt GroEL (1XCK, Bartolucci et al., 2005; PDB code 1XCK), of GroEL–GroES-$(ADP)_7$ complex (1AON, Xu et al., 1997; PDB code: 1AON), and of the DM GroEL R13G, A126V (1OEL, Braig et al., 1994; PDB code 1OEL). This last structure, despite preserving the inter-ring interface contacts observed in wt GroEL (Sewell et al., 2004), displays an altered allosteric behaviour (Aharoni and Horovitz, 1996), as it does $GroEL_{E461K}$ (Sot et al., 2002; Sewell et al., 2004).

The crystal structure of $GroEL_{E461K}$ has been determined by molecular replacement (3.3 Å resolution) with a crystallographic *R*-factor of 27.6% and a R_{free}-factor of 29.6% (Table 1). Residue 1 and the amino acid segment 526–547 are not included in this model since no interpretable density for these residues was found. The asymmetric unit (a.u.) in the C2221 space group corresponds to two identical rings brought into contact *via* the apical domains. Therefore, in the crystal

Fig. 2. Connections between inter-ring contacts and the $GroEL_{E461K}$ ATP-binding site. Two facing monomers from the top and bottom rings are shown. Amino-acids belonging to the *right* and *left* contact regions are coloured blue and yellow, respectively (see Table 3). The rings display a 1:1 subunit interaction or *in-register* assembly. Some of the amino-acids belonging to the ATP-binding site (ATP_{bs}) entrance are coloured red. The ATP_{bs} is connected to both inter-ring contact regions through a net of helices formed by helix O (aa 434–446), helix P (aa 449–457), and helix Q (aa 462–471). Salt-bridge Lys 470-Glu 448 (red circle) links the end of helix Q to helix O and helix P, which in turn connects helix Q with the nucoletide-binding pocket. Monomer domains are indicated **Ap** for apical, **Int** for intermediate, and **Eq** for equatorial. *Inset*: In 1XCK the interface is formed by a 1:2 subunit interaction. Monomers from different rings interact *left*-to-*left* and *right*-to-*right*, as they do in 1OEL and 1AON structures.

Fig. 3. Detail of the $GroEL_{E461K}$ inter-ring interface. Lysines 461 belonging to opposite rings accommodate their side-chains between two adjacent monomers as is shown by the average conformation in this figure (see text). This fitting functions as a steric mechanism that clamps ring rotation (see Section 3.3). Pro 462 and hydrogen bond between atoms O-461 and N-465 (dashed yellow line) restrain the main chain conformation of residue 461 (Glu in wt GroEL and Lys in $GroEL_{E461K}$), thereby pointing its side-chain to the inter-ring region. Green and gray surfaces correspond to two adjacent monomers of the top ring and grey and green *tubes* to main chain of two monomers in the bottom ring. For simplicity, only a few amino acids, in the form of a stick model, are included. *Inset*: Rectangled dashed zone corresponds to main image. 2EU1 monomer association is 1:1 or *in-register* alignment.

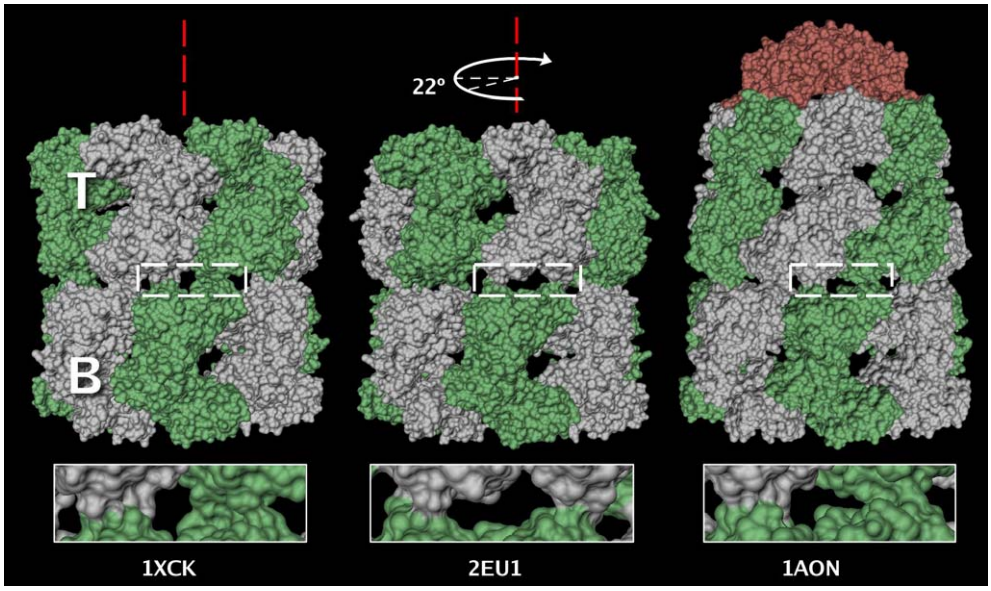

Fig. 1. Overall structure comparison of wt GroEL, the complex GroEL–GroES-$(ADP)_7$ and $GroEL_{E461K}$. GroEL consists of two stacked heptameric rings (top T and bottom B), each made of seven identical subunits (grey and green) related by a 7-fold symmetry axis (shown as dashed red lines). Upon nucleotide binding, wt GroEL binds GroES co-chaperonin (in red, on top of 1AON). In both wt GroEL (1XCK) and the complex GroEL–GroES-$(ADP)_7$ (1AON), each monomer contacts two monomers of the opposite ring; this is designated as a 1:2 subunit interaction. In $GroEL_{E461K}$ (2EU1), the T-ring is rotated 22° about the 7-fold axis (white arrow) in such a way that each monomer contacts only one monomer of the opposite ring in the so called 1:1 subunit interaction. The contact regions between the two rings (corresponding to one monomer at the B-rings) are enlarged and shown in rectangles.

structure the biological molecule is formed by two halves of neighbouring asymmetric units (each containing one GroEL ring), these ring being related by one of the crystallographic 2-fold symmetry axes. In this association, the buried surface

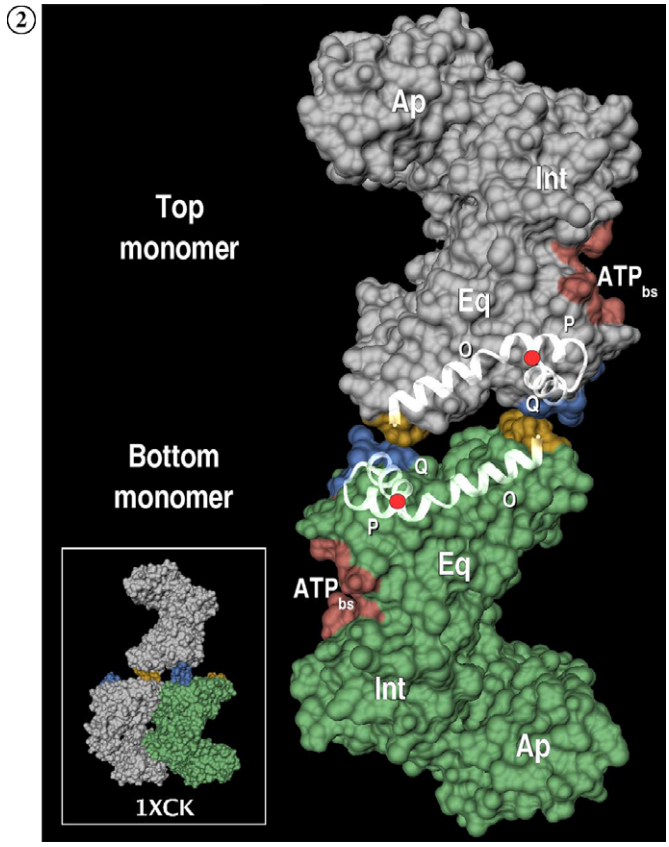

corresponding to equatorial domain contacts (2649.8 $Å^2$, Table 2) is 43% larger than that resulting from the apical domain contacts (1851.3 $Å^2$), indicating that inter-ring interaction through equatorial domains is stronger. We will therefore refer to the $GroEL_{E461K}$ structure (2EU1) as the association of two neighbouring rings related by 2-fold crystallographic symmetry, in agreement with the functional in-solution quaternary structure of GroEL.

All monomers in the 2EU1 crystallographic structure (termed A, B, C, D, E, F and G in one ring; H, I, J, K, L, M and N in the opposite ring) are almost identical. This becomes evident when any two of the 14 protein subunits are superimposed by their equivalent α-carbon atoms, yielding a small r.m.s.d. (Table 2). This high structural

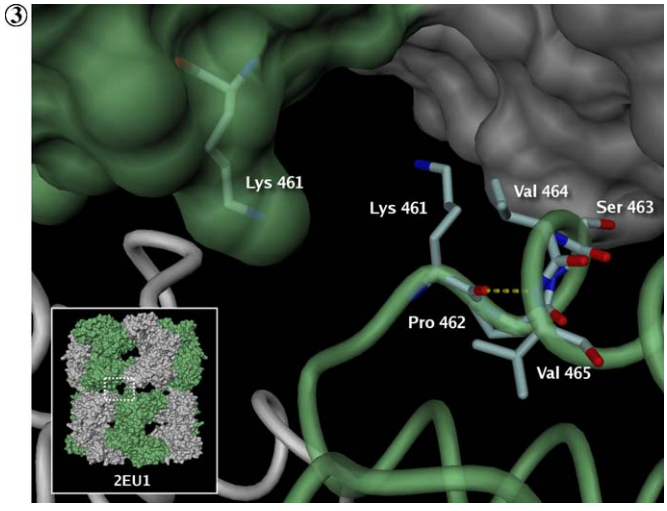

similarity among 2EU1 monomers can be a consequence of our limited data resolution and most likely to the fact that the apical domains do not display the rotational spread found in the *apo* structure of 1XCK (Bartolucci et al., 2005), as well as in the complexes DM-GroEL(ATP)$_{14}$ (Wang and Boisvert, 2003) and DM-GroEL(peptide)$_{14}$ (Wang and Chen, 2003). When a crossed-comparison, superimposing equivalent α-carbons between the average monomer of 2EU1 and that of 1XCK, is carried out, we observe that both structures are very similar (r.m.s.d. 0.5 Å). The only significant difference appears in an exposed loop (residues 310–314) where the α-carbon atoms at residue 311 are 1.8 Å apart.

Replacement of Glu 461 by Lys in wt GroEL hinders Glu 461-Arg 452 salt bridge formation, introducing a positively charged amino acid that modifies the surface charge distribution at the equatorial domain. Due to the nature of this mutation, we can expect an electrostatic repulsion between Lys 461 and Arg 452 to occur if the rings associate in the same way as they do in the 1XCK structure. Despite the perturbation caused by the mutation, the overall ring attraction remains sufficiently strong to force 2EU1 heptamers to adopt a quaternary arrangement compatible with the double-ring structure assumed in solution.

When the overall 2EU1 structure is compared with the 1XCK structure, two major changes are observed. Firstly, the two 2EU1 rings are rotated about their respective ring axis in such a way that each monomer contacts only one monomer of the opposite ring (Fig. 1). This ring assembly was found in the crystallographic structure of the thermosome and was designated as a 1:1 subunit interaction (Ditzel et al., 1998). The second global change is an increase in the inter-ring spacing (Table 2), that weakens inter-ring communication, an observation we had already reported for both this and the GroEL$_{E434K}$ mutant (Sot et al., 2002). Computation of the rigid body rotation of opposite rings by superimposition of equivalent α-carbons results in a rotation angle of approx. 22° around the 7-fold axis. This quaternary structural change was clearly observed on cryo-TEM images by Sewell et al., who gave an estimate of 18° for this rotation, which would also bring the rings *in-register* (Sewell et al., 2004). Based on this estimation, the authors predicted a new inter-ring interface featuring three inter-ring salt bridges: two between the pairs Glu 434-Lys 470, and a third one between one of the pairs Glu 102-Lys 105 (Sewell et al., 2004). Under our experimental conditions, however, none of these contacts occur. Even more surprisingly, no single salt-bridge is observed at the 2EU1 inter-ring interface. As it will be discussed below, we cannot rule out the possibility that an increase in temperature, in concert with less stringent in-solution conditions, might modify this situation.

The crystallographic structure of GroEL$_{E461K}$ reported in this study allows the computation of the distance between the center-of-mass of the equatorial domains of facing rings which turns out to be 0.7 Å larger in 2EU1 than in 1XCK (Table 2). On the other hand, when a probe sphere of 2.11 Å radius size is employed to compute the inter-ring buried surface in the 2EU1 structure, the estimated area (5247.7 Å^2) is similar to that of 1XCK when computed with a 1.4 Å-radius probe sphere (see Table 2). This is expected if the separation between the equatorial domain's center-of-mass of the two ring increases by 0.7 Å. The inter-ring distance separation between 2EU1 heptamers is further discussed in Section 3.4.

3.2. Stability of the GroEL$_{E461K}$ interface

Using the crystallographic structures of GroEL$_{E461K}$ and the above-mentioned references (1XCK, 1AON, and 1OEL), we quantified the stability of the ring interface, which would control inter-ring distance, in terms of the buried surface between the two rings. Computation of these surfaces showed that increasing ring separation allowed the solvent to access a larger inter-ring area in GroEL$_{E461K}$, as compared with the other two *apo* GroEL forms, and the GroEL–GroES-(ADP)$_7$ complex (Table 2). This solvation increase in 2EU1 corresponds to an inter-ring interaction energy decrease of about 200 KJ mol^{-1}, as can be estimated from the inter-ring interaction energy of the mutant and either of the two other *apo* molecules indicated in Table 2. This energy decrease is a direct consequence of the E461K mutation.

Based on the 1XCK and 1OEL structures, ring association in GroEL was believed to be stabilized by a few hydrogen bonds and a major interaction resulting from the hydrogen bond between Arg 452 and Glu 461 (Braig et al., 1995; Bartolucci et al., 2005). Additional contributions were also thought to come from residues Ser 463, Val 464 and Asn 467 (Braig et al., 1995). It has also been shown that the *influence* of each residue on the surrounding medium extends up to 8 Å (Manavalan and Ponnuswamy, 1977; Gromiha and Selvaraj, 2000; Jiang et al., 2002). If we regard such influence as *contact*, we can analyse the interaction between monomers in a more general way, rather than simply considering hydrogen bonds and van der Waals interactions. By computing the inter-atomic distances within a cut-off of 8 Å from one GroEL ring to the facing ring, we find that the number of contacts vary according to the allosteric state of GroEL (Table 2). Many contacts contribute to inter-ring interactions and a detailed description of the interacting amino acids is listed in Table 3. Interestingly, despite the decreased inter-ring buried surface in GroEL upon GroES and nucleotide binding, we observe that the number of contacts at the 1AON interface has increased (Tables 2 and 3). Furthermore, in 1XCK, 1OEL and 1AON, each monomer contacts two monomers from the facing ring, representing a 1:2 subunit interaction. This ring association puts into contact equivalent monomer regions, which are *left*-region to *left*-region, and *right*-region to *right*-region (Table 3). In contrast to what happens in these structures, aside from few long range interactions, each

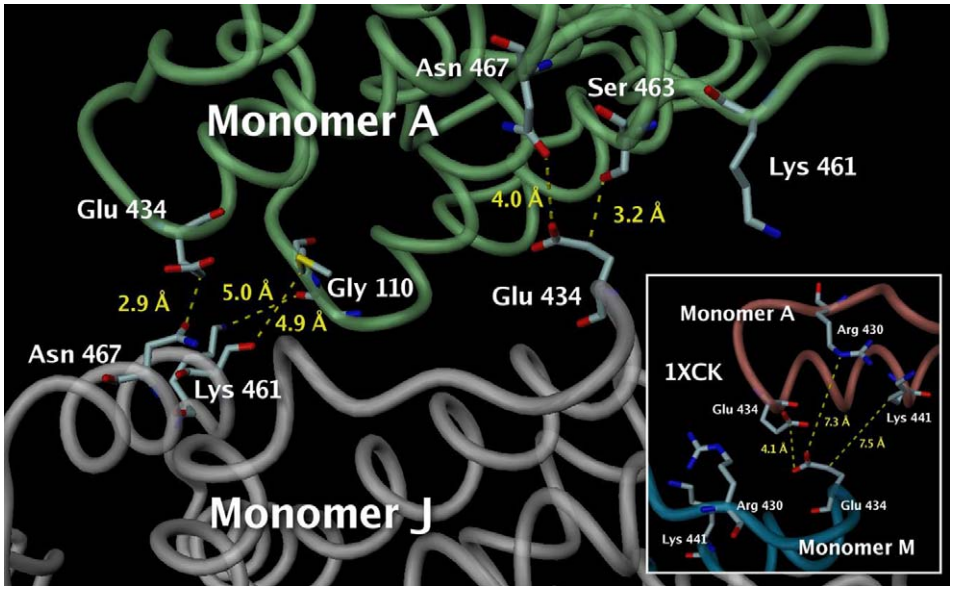

Fig. 4. Detail of $GroEL_{E461K}$ inter-ring contacts. In the crystallographic structure of $GroEL_{E461K}$ each monomer from one ring faces only one monomer from the opposite ring (for example monomers A and J in this figure). The short distances between atom CG-434 and OD1-467 (2.9 Å), and between OG-463 and CG-434 (3.2 Å), indicate that a strong interaction occurs in both contacting regions (see Section 3.3). In both opposing monomers, the side chain of Glu 434 has a conformation incapable of forming strong interactions with amino acids from the opposite ring. Nevertheless, if the inter-ring distance increases, this situation can change, allowing this glutamic residue to hydrogen bond or salt bridge amino acids beyond the inter-ring solvent space. The *tubes* sketch displays the main chain of facing monomers A and J. With the exception of Lys 461, which is shown for reference, stick models of all residues making inter-ring contacts at distances up to 5.0 Å apart were included. *Inset*: Glu 434 at the *left* contact site in 1XCK displays a folded conformation as found in 2EU1.

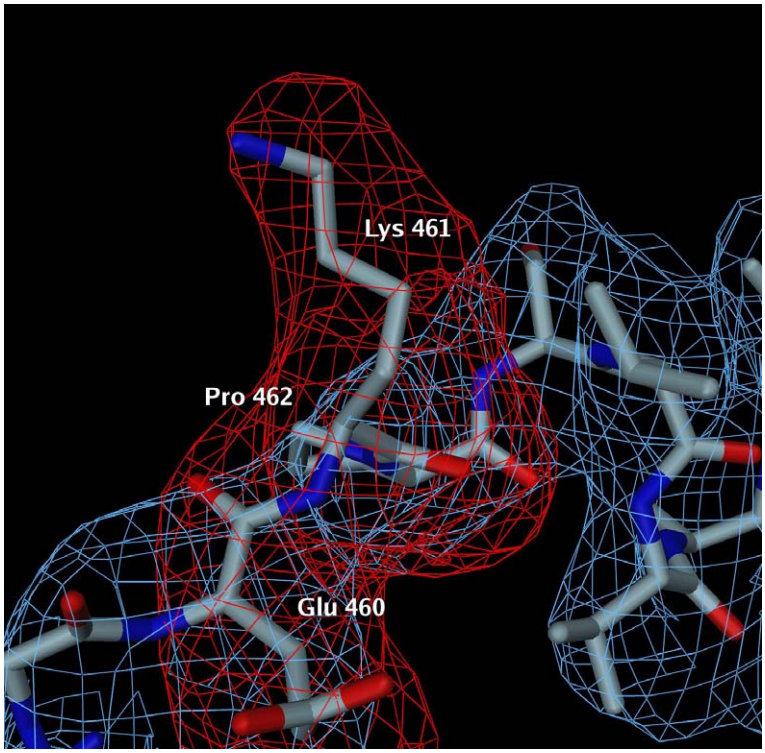

Fig. 5. Lysine 461 in $GroEL_{E461K}$ structure. The mutated residue is exposed to the solvent at the interface between rings. In this figure the conformation of residues 460–462 corresponds to the average conformation (after superposition by their equivalent CA-atoms) of the seven monomers A–G (see text). Averaged F_o–F_c density simulated annealed omit map of residues Glu 460–Pro 462 is coloured in red and contoured at 7σ. This omit map clearly shows Lys 461 extending its side chain to the inter-ring space. The blue map is an averaged $2F_o$–F_c density omit map (with phases computed without aa 460–462) contoured at 1.2σ.

Table 2
Numerical comparison between structures wt GroEL (1XCK), GroEL double mutant (1OEL), complex GroEL–GroES-$(ADP)_7$ (1AON) and single mutant $GroEL_{E461K}$ (2EU1)

	Cα atoms r.m.s.d. (equivalent monomers, Å)	Inter-ring buried surface (Å^2)	Number of inter-ring contacts (<8 Å)	Inter-ring interaction energy (kJ mol^{-1})	Inter-ring equatorial domain CCMM distance (Å)
1XCK	0.6	5147.8	743 (14)	411.8	33.0
1OEL	0.4	5166.5	786 (14)	413.3	32.7
1AON	0.2 (*cis*) 0.3 (*trans*)	4715.4	824 (7)	377.2	32.0
2EU1	0.1	2649.8	366 (0)	212.0	33.7

r.m.s.d. were computed between α-carbon atoms of equivalent monomers: 14 for 1XCK, 1OEL and 2EU1, and 7 for the *cis* and *trans* ring in 1AON. Buried surface (using a probe radius of 1.4 Å) and inter-atomic contacts were computed using the CNS program (Adams et al., 1997). Numbers in parenthesis correspond to number of inter-ring salt bridges. Inter-ring interaction energy was estimated as the product of the buried surface and the mean energy per unit area, based on a parameter value of 80 J mol^{-1} Å^{-2} (Richards, 1985). This interaction energy in 2EU1 is about 50% of those found for the other two *apo* forms (1XCK and 1OEL). Inter-ring equatorial domain CCMM distance refers to the distance between the center-of-mass of the two groups of seven equatorial domains belonging to each GroEL ring. These distances were computed with the program *lx_moleman* (Kleywegt, 1992–2005) taking solely protein atoms.

monomer in $GroEL_{E461K}$ establishes contacts mainly with one monomer from the opposite ring (Table 3). Thus, in 2EU1 a 1:1 subunit interaction or *in-register* ring assembly occurs at the inter-ring interface (Figs. 1 and 2). Also, due to the relative rotation between rings the contacting regions through the ring-interface is now arranged in the way all *left*-regions always face *right*-regions (Fig. 2). Note that we define contacting region as the group of residues of one monomer that contact another subunit at the opposing ring, instead of all aminoacids from opposing monomers that are at contact distance (Braig et al., 1994).

3.3. Structure of the $GroEL_{E461K}$ interface

GroEL inter-ring salt bridges Glu 461-Arg 452 (two per monomer in both 1XCK and 1OEL, and only one in 1AON; Table 3) are important not only to stabilize the inter-ring interface, but also to allow productive inter-ring communication (Sot et al., 2002; Sot et al., 2003). These ionic-contacts are formed because the side chains of both amino acids are oriented towards their partner amino acids beyond the inter-ring space. This is possible because Glu 461, which is located at the beginning of a helical segment of the equatorial domain, has the side chain protruding from the ring surface to the solvent of the inter-ring space. The orientation of the Glu 461 side chain is restrained by two neighbouring residue interactions: Pro 462 which imposes rigidity to the chain, and the hydrogen bond between atoms O-461 and N-465. In 2EU1 the same interactions restrain the main chain conformation of Lys 461, allowing its side chain to point outward the inter-ring solvent space (Fig. 3).

As mentioned before, no salt-bridges are observed at the $GroEL_{E461K}$ inter-ring interface, a finding which prompts the following question: how does the interaction between rings cause the interface following the mutation to reorganise in a specific way? Obviously, the interactions at the mutant's inter-ring interface must balance the electrostatic repulsion generated by the mutation, since the attractive force driving ring association stabilizes the double-ring structure of this protein at physiological temperatures (Sot et al., 2002). The equilibrium between attractive and repulsive forces in the 2EU1 ring association is partially balanced by increasing the inter-ring distance. This structural characteristic of the mutant will be discussed in the next section.

Due to the position and side chain orientation of Lys 461, this residue is the most contacting amino-acid at the mutant inter-ring interface (Table 3). Also, each lysine 461 from one ring fits in the space between two monomers of the opposite ring (Fig. 3). Due to the absence of inter-ring salt-bridges, this fitting might function as a "clamp mechanism" for the rotation that places the two rings into an *in-register* alignment (Figs. 2 and 3, inset). Interestingly, a similar interaction is found at the *left* site of 1XCK in which the most contacting residue, Ala 109 (Table 3), fits into a small concave space at the opposing subunit, this being the depression in the groove of the last turn of helix D (residue 87–109).

Glu 434 is the main contacting residue at the left contact region in the $GroEL_{E461K}$ structure (Table 3). This residue is located at the extreme of helix O (residues 434–446) and exposed to the inter-ring space (Fig. 4). A detailed analysis of averaged difference Fourier (F_o–F_c) and *omit* maps (calculated from a protein model excluding residues 432–436) shows a density that could not be modelled by arrangement of the side chain of residues Glu 434 closer to the opposite ring. All attempts to improve the fit were changed automatically after refinement by moving the side chain out of the electron density. Although the refinement procedure yields a model in which Glu 434 displays good stereochemical parameters, the manually fixed but slightly distorted starting model gave featureless difference Fourier maps (data not shown). In the final model the side-chain of Glu 434 in all monomers is folded back as a consequence of steric hindrance with residues of the facing ring, as shown for the monomer A in Fig. 4. Some of the inter-atomic distances at the ring-interface are smaller than the corresponding addition of the radii of the pair of atoms involved in the contact. An example of these short distances is 2.9 Å between OD1-

467 and CG-434 (Fig. 4), where the minimum value for the sum of the corresponding standard atomic radii of these two atoms is 3.2 Å (Gerstein et al., 2001). These inter-ring contacts are interpreted as a *clash* between the two heptamers due to the association force that remains strong even in the absence of salt-bridges found in all GroEL structures (1XCK, 1OEL and 1AON). This disk association is further analysed in the next section.

3.4. GroEL$_{E461K}$ temperature sensitivity and inter-ring distance

In our previous studies on GroEL$_{E461K}$ it was assumed that the mutation did not introduce any further structural changes other than the corresponding inter-ring salt bridge disruption (Sot et al., 2002, 2003). The structure of GroEL$_{E461K}$, initially at low resolution (Sewell et al., 2004) and in this study at atomic detail, reveals that together with inter-ring salt bridge disruption, two other major quaternary structural changes occur: ring separation and solid ring rotation. Therefore, all the experimental findings obtained to date must be re-interpreted in terms of a remodelled scenario in which inter-ring distance and ring rotation are new factors affecting allosterism and thermal sensitivity.

Regarding the stability of the double-ring assembly, the structure described in this study provides a solid basis to understand the decreased thermal stability of GroEL$_{E461K}$ observed in DSC and in thermal inactivation experiments (Sot et al., 2003). It is particularly interesting to note the strong correlation found between the decrease of both the inter-ring interaction energy (estimated from the 3D structure of GroEL$_{E461K}$ to be ≈50%; Table 2), and the activation energy of denaturation obtained from DSC and inactivation experiments (≈40%; Sot et al., 2003). This finding suggests that interactions at the protein's inter-ring interface are important factors in determining the stability and functional properties of the tetradecameric protein particle.

Another important factor that can be further analysed is the effect of temperature on the functional properties of wt GroEL and GroEL$_{E461K}$. This single point mutation abolishes the ability of this protein to refold protein substrates in a temperature-dependent manner; e.g., it refolds denatured malate dehydrogenase at 25 °C but not at 37 °C, although it binds it at both temperatures (Sot et al., 2002). This finding, together with other experimental evidences indicating that negative inter-ring communication was weaker (Llorca et al., 1998; Sot et al., 2002) and inter-ring spacing larger over increasing temperatures (Sot et al., 2002), suggested that increased distance between protein rings impaired inter-ring communication and thus substrate dissociation from the chaperonin (Sot et al., 2002). The midpoint temperature at which this behaviour occurred was shown to be 7 °C lower for GroEL$_{E461K}$ than for the wt protein (Sot et al., 2003). The data presented here support the interpretation that the increased inter-ring spacing observed in the single point mutant, as compared with 1XCK, arises from the formation of a double-ring assembly that is weaker and that has an inter-ring interface more accessible to the solvent.

Our recent spectroscopic study of wt GroEL and several mutants, including GroEL$_{E461K}$, revealed the presence of electrostatic interactions at the inter-ring interface of GroEL$_{E461K}$ that were sensitive to ATP binding (Sot et al., 2005). However, we did not find any evidence of an inter-ring salt bridge in the 3D structure of GroEL$_{E461K}$ protein at 4 °C. One way to explain this apparent contradiction would be to assume that an increase in temperature would, as suggested in solution over the 25–45 °C temperature range by EM (Llorca et al., 1998; Sot et al., 2002), increase the inter-ring distance. This could rearrange residues from opposite rings, favouring the formation of inter-ring salt bridges that did not occur in the 4 °C-crystallographic structure. One of these potential contacts could be a salt-bridge between Lys 461 and Glu 434 (Fig. 4), which might stabilize the double-ring conformation in the same way salt-bridge Arg 452–Glu 461 does in 1XCK (Braig et al., 1995). Moreover, if the salt-bridge Glu 434–Lys 461 does form, it would be sensitive to ATP-binding since both residues are connected to the ATP-binding site through a net of helices (O, P and Q, Fig. 2), thereby explaining the signal observed at 25 °C in our time-resolved infrared difference analysis (Sot et al., 2005).

3.5. Inter- and intra-ring signalling in GroEL$_{E461K}$

In vitro measurement of ATPase activity of GroEL$_{E461K}$ revealed the loss of both positive and negative co-operativities at physiological and stress temperatures (Sot et al., 2002; Sewell et al., 2004). This defective behaviour can be attributed to the mutant inter-ring interface as a consequence of this single residue replacement.

To discuss this finding it has to be kept in mind that the route of allosteric signalling in GroEL is not completely understood and signal transmission is associated to both steric clashes through *en bloc* movements and to conformational changes within protein domains. From the comparison of the available structures of GroEL complexed with different ligands (Xu et al., 1997; Wang and Boisvert, 2003), and the analysis of correlated mutations (Kass and Horovitz, 2002), several structural regions have been proposed to participate in the transmission of the inter-ring allosteric signal (Ranson et al., 2001; Sewell et al., 2004; Bartolucci et al., 2005). Among them, distortions transmitted through helix D (residues 87–109) might provide leverage for equatorial domain tilting (Sewell et al., 2004). A recently proposed movement of the stem loop (residues 34–52) upon ATP binding would favour formation of new contacts in which these residues can be involved. Interestingly, this conformational change could induce the asymmetry found for the salt-bridge Arg 452–Glu 461, the stronger interaction present at the inter-ring interface. Such an effect has been related to the ability of ATP and ADP–GroES

Table 3
GroEL inter-ring interface contacts (distance < 8 Å): Number of contacts that residues at the top ring establish with aminoacids at the bottom ring

Residue	1XCK		1OEL		1AON-*cis*		1AON-*trans*		2EU1	
	L	R	L	R	L	R	L	R	L	R
Left region										
Asn 10			5		21					
Val 14					9					
Leu 17					7					
Thr 101	3		5		14					
Glu 102	21		23		21		21		3#	
Gly 103					2					
Leu 104	7		7		21					
Lys 105	49		54		76		27		9#	
Ala 106	34		35		26		21			5
Val 107	14		14		14		7			2
Ala 108	35		34		63		28			2
Ala 109	76		75		81		81		2#	17
Gly 110	36		37		35		43			12
Met 111	37		43		30		51			17
Asn 112					7		7			6
Leu 116										
Arg 430	7		7				7			2
Gln 432										1
Asn 433										14
Glu 434	38		43		24		98			48
Asp 435	1		7		7		14			18
Asn 437	7		7		7		10			10
Val 438	25		21		7		36			13
Gly 439					7					
Lys 441	7		7		7		21			
Val 442					7		7			
Arg 445	14		21		7		21		2#	
Right region										
Glu 448		7		7				7	1	
Arg 452		14 (7)		21 (7)		21		21 (7)	9	
Leu 456									2	
Gly 459									4	
Glu 460		6		2		14			7	
Glu 461[a]		63 (7)		65 (7)		77 (7)		42	44	9#
Pro 462		21		21		21		21	10	
Ser 463		47		46		42		56	34	
Val 464		63		63		63		53	24	
Val 465		21		25		21		28	4	
Ala 466		14		14		4		14	3	
Asn 467		48		44		42		49	25	
Thr 468		14		19		12		26	4	
Lys 470		7		7				7	3	
Tyr 485		7		7		7				
Total site	**411**	**332**	**445**	**341**	**478**	**346**	**500**	**324**	**190**	**176**
Total	**743**		**786**		**824**		**824**		**366**	

Left (L) and Right (R) regions on each monomer of wt GroEL (1XCK), of the double mutant (1OEL) and of the complex GroEL–GroES-$(ADP)_7$ (1AON), interacts with L and R regions, respectively, of two adjacent monomers of the opposite ring. This 1:2 subunit interaction brings equivalent monomer regions into contact, i.e., 'L-to-L' and 'R-to-R' (see *inset* in Fig. 2). In $GroEL_{E461K}$ (2EU1) each monomer interacts mainly with one monomer of the opposite ring and weakly with the two adjacent monomers of the main contacting subunit (these contacts are indicated with # in columns 10 and 11). Therefore, in 2EU1 inter-ring contact can be regarded as a 1:1 subunit interaction or *in-register* assembly. Salt-bridge numbers are shown in parenthesis. r.m.s.d. were computed between α-carbon atoms of equivalent monomers: 14 for 1XCK, 1OEL and 2EU1, and 7 for the *cis* and *trans* ring in 1AON. Buried surface (using a probe radius of 1.4 Å) and inter-atomic contacts were computed using the CNS program (Adams et al., 1997). Numbers in parenthesis in the fourth column correspond to the number of inter-ring salt bridges. Inter-ring interaction energy was estimated as the product of the buried surface and the mean energy per unit area, based on a parameter value of 80 J mol^{-1} $Å^{-2}$ (Richards, 1985). This interaction energy in 2EU1 is about 50% of those found for the other two *apo* forms (1XCK and 1OEL). Inter-ring equatorial domain CCMM distance refers to the distance between the center-of-mass of the two groups of seven equatorial domains belonging to each GroEL ring. These distances were computed with the program *lx_moleman* (Kleywegt, 1992–2005) taking solely protein atoms.

[a] In 2EU1 residue 461 is Lys.

to induce a *trans* to *cis* conformational transition in Leu 31, that would promote intra-subunit and inter-ring rearrangements (Bartolucci et al., 2005). The interaction of the γ-phosphate of the nucleotide with atom N-Gly32 would stabilize the *cis* conformation of Leu 31, by locking several residues of this loop. This increase in rigidity can be transmitted to helix P, where Arg 452 is located, and helix Q, which holds Glu 461, therefore changing the structural properties of the inter-ring interface of the complexes with ATP and ADP–GroES, as compared with that of the *apo*-protein (Bartolucci et al., 2005).

A similar analysis of the *apo*-form of $GroEL_{E461K}$ reveals that Leu 31 adopts only the *cis* conformation, which seems to be stabilized by two hydrogen bonds between atoms ND2-Asn 457 and O-Lys 28, and ND2-Asn 457 and O-Leu 31, with average distances of 3.3 Å and 2.8 Å, respectively. As in the *cis*-ring of the GroEL–GroES-$(ADP)_7$ (1AONcis; Xu et al., 1997) and the DM-GroEL-$(ATP)_{14}$ (1KP8; Wang and Boisvert, 2003) structures, in 2EU1 atoms O-Gly 32 and N-Gly 35 are hydrogen bonded, with the average distance of this contact being 2.8 Å (2.8 Å in 1AONcis and 2.9 Å in 1KP8), shorter than that found in 1XCK (3.2 Å, Bartolucci et al., 2005). This finding suggests that the region around Leu 31 is more structured in the mutant than in 1XCK, similar to what is found in both 1AONcis and 1KP8 structures. Considering flexibility as the main factor affecting the conformation of Leu 31, it can be proposed that rigidification of this protein region as a consequence of the E461K mutation could lead Leu 31 to adopt only the *cis* conformation in 2EU1, with the subsequent weakening of intra-ring signalling.

Acknowledgments

We thank J. Navaza for help in using AMoRe, as well as I. Fita, F.M. Goñi, and C. Cambillau for critical assessment of the manuscript. A.C.-B. and J.A. are recipients of fellowships from the Basque Government and A.M.-G. from the MEyC, Spain. We also thank the ESRF and members of the ID29 staff for support and assistance in data collection. Part of this work was funded by ETORTEK, FEDER, MEC (BFU2004-03452/02955), and UPV/EHU (13505/2001).

References

Adams, P.D., Pannu, N.S., Read, R.J., Brunger, A.T., 1997. Cross-validated maximum likelihood enhances crystallographic simulated annealing refinement. Proc. Natl. Acad. Sci. USA 94, 5018–5023.

Aharoni, A., Horovitz, A., 1996. Inter-ring communication is disrupted in the GroEL mutant Arg 13 → Gly; Ala 126 → Val with known crystal structure. J. Mol. Biol. 258, 732–735.

Bartolucci, C., Lamba, D., Grazulis, S., Manakova, E., Heumann, H., 2005. Crystal structure of wild-type chaperonin GroEL. J. Mol. Biol. 354, 940–951.

Braig, K., Otwinowski, Z., Hedge, R., Boisvert, D.C., Joachimiak, A., Horwich, A.L., Sigler, P.B., 1994. The crystal structure of the bacterial chaperonin GroEL at 2.8 Å. Nature 371, 578–586.

Braig, K., Adams, P.D., Brunger, A.T., 1995. Conformational variability in the refined structure of the chaperonin GroEL at 2.8 Å resolution. Nat. Struct. Biol. 2 (12), 1083–1094.

Brunger, A.T., Adams, P.D., Clore, G.M., DeLano, W.L., Gros, P., Grosse-Kunstleve, R.W., Jiang, J.S., Kuszewski, J., Nilges, M., Pannu, N.S., Read, R.J., Rice, L.M., Simonson, T., Warren, G.L., 1998. Crystallography & NMR system: A new software suite for macromolecular structure determination. Acta Crystallogr. D., Biol. Crystallogr. 54, 905–921.

Collaborative Computational Project, Number 4, 1994. The CCP4 Suite: Programs for Protein Crystallography. Acta Cryst. D 50, 760-763.

Ditzel, L., Lowe, J., Stock, D., Stetter, K.O., Huber, H., Huber, R., Steinbacher, S., 1998. Crystal structure of the thermosome, the archaeal chaperonin and homologue of CCT. Cell 93, 125–138.

Gerstein, M., Richards, F.M., Chapman, M.S., Connolly, M. L., 2001. Molecular geometry and features in International Tables for Crystallography, F., 531–545.

Gromiha, M.M., Selvaraj, S., 2000. Inter-residue interactions in the structure, folding, and stability of proteins. Res. Dev. Biophys. Chem. 1, 1–14. Recent Research.

Inobe, T., Kikushima, K., Makio, T., Kuwajima, K., 2003. The allosteric transition of GroEL induced by metal fluoride-ADP complexes. J. Mol. Biol. 23 (329(1)), 121–134.

Jiang, Z., Zhang, L., Chen, J., Xia, A., Zhao, D., 2002. Effect of amino acid on forming residue–residue contacts in proteins. Polymer 43, 6037–6047.

Jones, T.A., Zou, J.Y., Cowan, S.W., Kjeldgaard, M., 1991. Improved methods for building protein models in electron density maps and the location of errors in these models. Acta Crystallogr. A47, 110–119.

Kass, I., Horovitz, A., 2002. Mapping pathways of allosteric communication in GroEL by analysis of correlated mutations. Proteins: Struct. Funct. Genet. 48, 611–617.

Kleywegt, G.J., 1992–2005. Uppsala University, Uppsala, Sweden. Uppsala Software Factory. Http://xray.bmc.uu.se/usf.

Lee, B., Richards, F.M., 1971. The Interpretation of Protein Structures: Estimation of Static Accessibility. J. Mol. Biol. 55, 379–400.

Llorca, O., Marco, S., Carrascosa, J.L., Valpuesta, J.M., 1994. The formation of symmetrical GroEL–GroES complexes in the presence of ATP. FEBS Lett. 345 (2–3), 181–186.

Llorca, O., Galán, A., Carrascosa, J.L., Muga, A., Valpuesta, J.M., 1998. GroEL under heat-shock. Switching from a folding to a storing function. J. Biol. Chem. 273, 32587–32594.

Manavalan, P., Ponnuswamy, P.K., 1977. A study of the preferred environment of amino acid residues in globular proteins. Arch. Biochem. Biophys. 184, 476–478.

Martin, A., Toselli, E., Rosier, M., Auffray, C., Devignes, M., 1995. Rapid and high efficiency site-directed mutagenesis by improvement of the homologous recombination technique. Nucleic Acids Res. 23, 1642–1643.

Navaza, J., 1994. AmoRe: an automated package for molecular replacement. Acta Crystallogr. A50, 157–163.

Otwinowky, Z., Minor, W., 1997. Processing of X-ray diffraction data collected in oscillation mode. Methods Enzymol. 276, 307–326.

Pérez-Pérez, J., Gutierrez, J., 1995. An arabinose-inducible expression vector, pAR3, compatible with ColE1-derived plasmids. Gene (Amst). 158, 141–142.

Ranson, N.A., Farr, G.W., Roseman, A.M., Gowen, B., Fenton, W.A., Horwich, A.L., Saibil, H.R., 2001. ATP-bound states of GroEL captured by cryo-electron microscopy. Cell 107, 869–879.

Richards, F.M., 1985. Calculation of molecular volumes and areas for structures of known geometry. Methods in Enzymology 115, 440–464.

Sewell, B.T., Best, R.B., Chen, S., Roseman, A.M., Farr, G.W., Horwich, A.L., Saibil, H.R., 2004. A mutant chaperonin with rearranged inter-ring electrostatic contacts and temperature-sensitive dissociation. Nat. Struct. Mol. Biol. 11, 1128–1133.

Sot, B., Galán, A., Valpuesta, J.M., Bertrand, S., Muga, A., 2002. Salt bridges at the inter-ring interface regulate the thermostat of GroEL. J. Biol. Chem. 277, 34024–34029.

Sot, B., Bañuelos, S., Valpuesta, J.M., Muga, A., 2003. GroEL stability and function. J. Biol. Chem. 34, 32083–32090.

Sot, B., Von Germar, F., Mantele, W., Valpuesta, J.M., Taneva, S., Muga, A., 2005. Ionic interactions at both inter-ring contact sites of GroEL are involved in transmission of the allosteric signal. A time-resolved infrared difference study. Protein Sci. 14 (9), 2267–2274.

Wang, J., Boisvert, D.C., 2003. Structural basis for GroEL-assisted protein folding from the crystal structure of (GroEL-KMgATP)14 at 2.0 Å resolution. J. Mol. Biol. 327, 843–855.

Wang, J., Chen, L., 2003. Domain motion in GroEL upon binding of an oligopeptide. J. Mol. Biol. 334, 489–499.

Weissman, J.S., Hohl, C.M., Kovalenko, O., Kashi, W.A., Chen, S., Braig, K., Saibil, H.R., Fenton, W.A., Horwich, A.L., 1995. Mechanism of GroEL action: productive release of polypeptide from a sequestered position under GroES. Cell 83, 577–588.

Xu, Z., Horwich, A.L., Sigler, P.B., 1997. The crystal structure of the asymmetric GroEL–GroES-$(ADP)_7$ chaperonin complex. Nature 388, 741–750.

Yifrach, O., Horovitz, A., 1995. Nested Cooperativity in the ATPase activity of the oligomeric chaperonin GroEL. Biochemistry 34, 5303–5308.